Distortion in Broad-Band Gallium Arsenide MESFET Control and Switch Circuits

Robert H. Caverly, *Member, IEEE*

Abstract—**This paper will discuss the origins of MESFET distortion in passive control applications, such as single transistor switch and reflective anttenuator circuits. The discussion is based on a lumped element equivalent circuit model and is limited to applications where the MESFET is operating in its conducting state. In switch circuits, the analysis indicates that distortion may be reduced by the use of MESFET's with pinch off voltages in the 2–3 V range and with large open channel current capacities. In attenuators, the analysis shows extreme variations in the level of distortion over a relatively narrow range of attenuation levels. Distortion in the case of the reflective attenuator may be reduced by the use of MESFET's with small open channel current capacities.**

I. Introduction

GALLIUM arsenide (GaAs) metal–semiconductor field effect transistors (MESFET's) offer significant advantages over conventional p-i-n diodes in many radio frequency (RF) and microwave switch and control applications. These advantages include low bias power consumption, the inherent bias isolation of the MESFET, and easy incorporation into monolithic circuits. The MESFET, however, has a specific nonlinear current–voltage characteristic. Thus, there will be harmonically related signals generated by the device when used as a control element. The interest in the distortion generated by MESFET control devices has become more significant recently with the increased use of monolithic MESFET control circuits in RF and microwave systems. In these applications, particularly in sensitive receivers where multiple signals are simultaneously received, the generation of in-band intermodulation signals can seriously affect receiver sensitivity. Similar concerns may be applied to phase shifter and signal routing applications.

A study by Gutmann and Fryklund [1] has shown that the GaAs MESFET exhibits significant nonlinearities at power levels less than 30 dBm. The investigators attribute the resistive nonlinearities to the onset of current saturation in the device. It is also expected that lower levels of nonlinearity will occur in the presaturation or the so-called linear region of operation. These nonlinearities in the conducting state resistance can affect circuit and system parameters such as insertion loss and distortion. More recent studies of GaAs MESFET control circuits by Gutmann and Jain [2], [3] have discussed significant implications in broad-band control circuits using MESFET's due to the gate bias circuitry. This gate bias network is also expected to influence the device and circuit nonlinearities. Absent in any of these works, however, has been a study of those device and circuit parameters that govern the level of distortion in single MESFET switch and control circuits.

This paper analyzes the nonlinear mechanisms of the MESFET in its passive control mode of operation, and equations are developed that will allow designers to predict second- and third-order harmonic and intermodulation products in the conducting state MESFET. The analytic expressions are verified by experimental data.

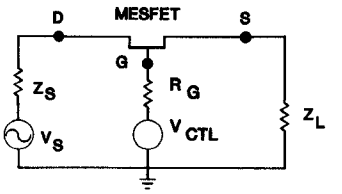

Fig. 1. A series connected MESFET used as a broad-band RF and microwave semiconductor control circuit element.

II. Theory and Analysis

A small-signal nonlinear model applicable to RF and microwave frequencies is necessary to determine the distortion characteristics of the MESFET. The basic circuit for the model, shown in Fig. 1, shows a series connected MESFET between a generator (V_S, Z_S) and a load (Z_L). Included in the circuit are the gate bias resistance (R_G) and the gate control voltage (V_{CTL}). Here, $Z_L = Z_S = Z_0$, where Z_0 is the characteristic impedance of the transmission line, which is assumed to be 50 Ω. Fig. 2 shows a simple ac equivalent circuit model for the GaAs MESFET in a typical broad-band control application. The nonlinear current–voltage relationship, $I_{DS} - V_{DS}$, and its relationship to the MESFET channel resistance R_{ch} needs to be determined to understand the distortion generated in the device. A general expression for the nonlinear I_{DS}–V_{DS} relationship may be placed in the form of a power series [4]:

$$I_{DS} = \sum_{n=1}^{\infty} \alpha_n V_{DS}^n \tag{1}$$

where the α_n describe the linear ($n = 1$) and nonlinear ($n > 1$) behavior of I_{DS}. The α_n may be found from the results of numerical simulations based on physical models [5], [6], or from closed-form expressions for the drain–source current using the gradual channel-abrupt depletion approxi-

Manuscript received July 9, 1990; revised December 4, 1990. The paper was supported by the National Science Foundation under Grant INT-8913608.

The author is with the Department of Electrical and Computer Engineering, Southeastern Massachusetts University, North Dartmouth, MA 02747.

IEEE Log Number 9143029.

0018-9480/91/0400-0713$01.00 ©1991 IEEE

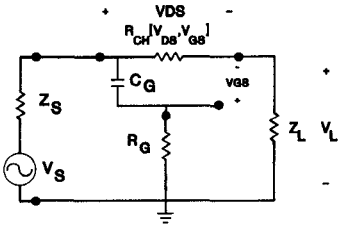

Fig. 2. The ac equivalent circuit of a MESFET used as a broad-band semiconductor control circuit element.

mations [7], [9]. In both cases, the α_n will include the effects of the gate bias voltage, V_{GS}, and the gate bias circuit composed of C_G and R_G.

From a study of Fig. 2, the gate capacitance C_G will affect the magnitude of the gate–source voltage as the frequency changes. This capacitance may be assumed constant, which is only true at low power levels. At high frequencies, the gate capacitance allows the gate to float and follow the drain. At lower frequencies, the gate capacitance's high impedance forces the gate to near RF ground, with the result that V_{GS} tracks with the load voltage V_L ($V_{GS} = -50\ I_{DS}$ {2}). The variation in V_{GS} will influence both the linear and the nonlinear characteristic of R_{ch}. This frequency dependence due to the gate bias circuit has been discussed in terms of the power handling capability of the MESFET by several investigators [3], [10]. From Fig. 2, V_{GS} may be written in terms of V_{DS} as

$$V_{GS} = -\frac{\left\{\frac{Z_0}{R_{ch}}\right\} - j\beta}{1 + j\beta} V_{DS} \tag{2}$$

where $\beta = \omega R_G C_G$.

Closed-form expressions for the α_n may be found by using a closed-form expression for the I_{DS}–V_{DS} characteristic, but now including the effects of the gate bias circuit through (2). Assuming uniform channel doping, use of the gradual channel approximation [7]–[9] and (2) allows one to write I_{DS} as

$$I_{DS} = I_P\left[\frac{3V_{DS}}{V_P} - 2\left\{\frac{V + (1+\gamma)V_{DS}}{V_P}\right\}^{1.5} + 2\left\{\frac{V + \gamma V_{DS}}{V_P}\right\}^{1.5}\right] \tag{3}$$

where γ is V_{GS}/V_{DS} (eq. (2)), I_P is related to the open channel current, V_P is the pinch off voltage, $V = V_{bi} - V_{GS0}$, V_{bi} is the built-in junction potential, and V_{GS0} is the dc gate bias voltage. The expression for I_{DS} in (3) is valid for V_{DS} less than the saturation voltage V_{DSAT}. This constraint limits the results of the model to small-signal levels where the peak RF voltage across the drain to source channel is less than V_{DSAT}. Using (3), the first three coefficients (α_n) of (1) may be written as

$$\alpha_1 = \frac{3I_P}{V_P}\left(1 - \sqrt{\frac{V}{V_P}}\right) \tag{4a}$$

$$\alpha_2 = -\frac{3I_P}{4V_P}\frac{1+2\gamma}{\sqrt{VV_P}} \tag{4b}$$

$$\alpha_3 = \frac{I_P}{8(VV_P)^{1.5}}(1 + 3\gamma + 3\gamma^2) \tag{4c}$$

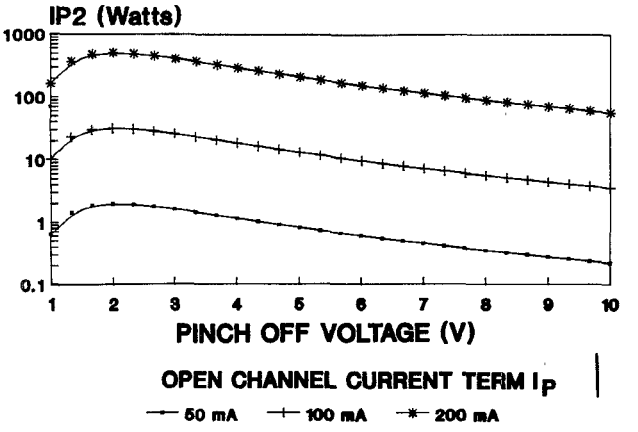

Fig. 3. Second-order intercept point (IP2) plotted versus pinch off voltage V_P with the open channel current term I_P as a parameter. The term γ is assumed to be unity.

where γ is a function of frequency (eq. (2)). Note that the channel resistance R_{ch} is the linear term in (1), $1/\alpha_1$.

The form for the nonlinear GaAs MESFET current given in (1) is applicable to any circuit containing one or more devices. A discussion of the distortion in single GaAs MESFET attenuators and switches (in the conducting state) in the presence of a single-tone RF signal follows. The discussion will be limited to second- and third-order distortion, but can be extended to higher order.

The single figure of merit commonly used as a measure of distortion is called the intercept point [11]. The intercept point is an extrapolation of the distortion power to the power level of the drive signal, assuming no compression of the drive signal. It is a fictitious power level, but provides a useful number from which distortion at any drive power may be derived [12]. For the single MESFET circuit shown in Fig. 1, the second (IP2) and third (IP3) order load intercept points may be written as:

$$\mathrm{IP2} = \frac{\alpha_1^4 Z_0}{2\alpha_2^2}(1 + 2Z_0\alpha_1)^2 \tag{5}$$

and

$$\mathrm{IP3} = \frac{\alpha_1^3 Z_0}{2\alpha_3}(1 + 2Z_0\alpha_1). \tag{6}$$

A. Switches

For switch circuits where R_{ch} is significantly less than Z_0, IP2 and IP3 may be written as

$$\mathrm{IP2} = \frac{2592 Z_0^3 V_{bi} I_P^4}{V_P^3}\left(1 - \sqrt{V_{bi}/V_P}\right)^6 / |1 + 2\gamma|^2 \tag{7a}$$

and

$$\mathrm{IP3} = \frac{648 Z_0^2 V_{bi}^{3/2} I_P^3}{V_P^{5/2}}\left(1 - \sqrt{V_{bi}/V_P}\right)^4 / |1 + 3\gamma + 3\gamma^2|. \tag{7b}$$

Figs. 3 and 4 show IP2 and IP3 plotted versus pinch off voltage V_P with the open channel current term I_P as a

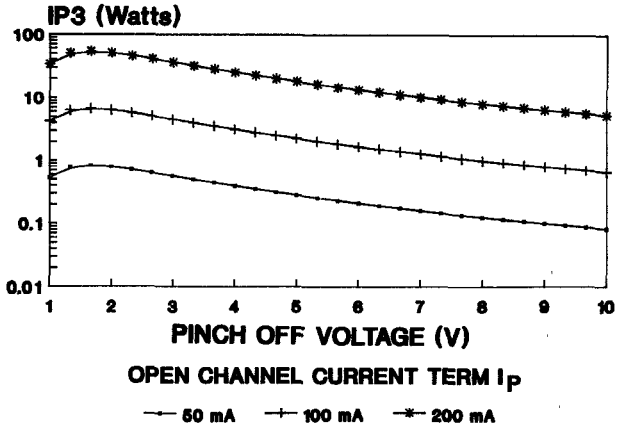

Fig. 4. Third-order intercept point (IP3) plotted versus pinch off voltage V_P with the open channel current term I_P as a parameter. The term γ is assumed to be unity.

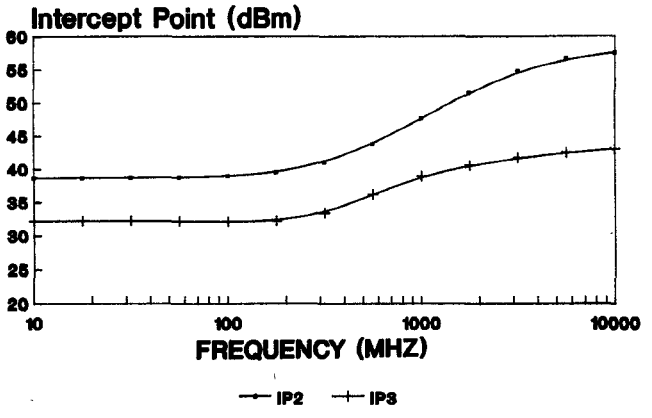

Fig. 5. Frequency dependence of the second- and third-order intercept points (IP2 and IP3) in a series connected switch. The MESFET exhibits a pinch off voltage of 2.5 V and an open channel current term of 200 mA. A gate resistance of 1 kΩ and a gate capacitance of 0.5 pF are assumed.

parameter for frequencies much greater than the gate circuit time constant ($\gamma = 1$). Note that there is a peak in the intercept point for pinch off voltages in the range of 2–3 V. The decrease in intercept point for pinch off voltages below approximately 2 V is due to the lowered value of V_{DSAT} in the device, with the resulting nonlinearities caused by operation near the onset of saturation [1]. Also, the intercept point increases with the open channel current term. I_P, and hence the intercept point, may be increased in a circuit by increasing the channel height or width, a condition consistent with improved power handling, switch Q, and conducting state resistance [1], [2], [13]. The distortion characteristics of the p-i-n diode exhibit a similar improvement with reduced forward bias resistance [12].

The frequency dependence of IP2 and IP3 is illustrated in Fig. 5 for a MESFET with a pinch off voltage of 2.5 V and an open channel current term of 200 mA, where the intercept point is plotted versus frequency. In this example, a gate resistance R_G of 1 kΩ and gate capacitance C_G of 0.5 pF are used. Note that there is a 20 dB increase in IP2 from its low frequency value. The rapid change in intercept point occurs in the vicinity of $1/2\pi R_G C_G$.

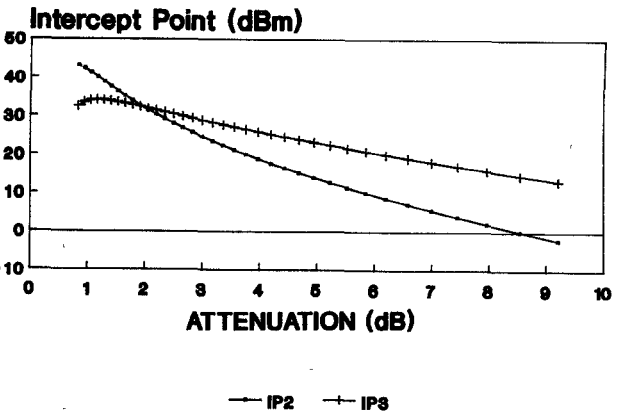

Fig. 6. Second- and third-order intercept point (IP2 and IP3, respectively) plotted versus attenuation (A) for a MESFET with a pinch off voltage of 2.5 V and an open channel current term of 200 mA. The frequency of operation is $1/2\pi R_G C_G$.

B. Attenuators

The identical circuit topology shown in Fig. 1 can be used as a reflective attenuator. In this case, the conducting state resistance R_{ch} is controlled by the gate bias voltage (V_{GS0}). If the level of attenuation is defined as

$$A = \left\{ \frac{2Z_0}{R_{ch} + 2Z_0} \right\}^2 \tag{8}$$

then IP2 and IP3 for the series reflective MESFET attenuator may be written as

$$\text{IP2} = \frac{A^2 V_P^3}{18 Z_0^3 I_P^2 \left(1 - \sqrt{A}\right)^6} (V_{bi} - V_{GS0}) / |1 + 2\gamma|^2 \tag{9a}$$

and

$$\text{IP3} = \frac{A^{3/2} V_P^{3/2}}{2 Z_0^2 \left(1 - \sqrt{A}\right)^4 I_p} (V_{bi} - V_{GS0})^{3/2} / |1 + 3\gamma + 3\gamma^2|. \tag{9b}$$

Here, improvements in attenuator distortion for a given V_{GS0} may be observed with MESFET's of low current handling capacity (small I_p). In the attenuator, relatively large values of conducting state resistance (up to several hundred Ω) may be required. The larger conducting state resistances may be achieved with lower channel dopings, narrower gate widths, and/or thinner channels, all yielding lower values of I_P and hence improved attenuator distortion performance. Fig. 6 shows IP2 and IP3 versus attenuation level (A) for a MESFET with pinch off voltage of 2.5 V and an open channel current term of 200 mA. Note the extreme range of intercept point from 0 to 10 dB attenuation. The low intercept point at the higher levels of attenuation can complicate the design of single MESFET low distortion attenuators.

III. Experimental Results

Second- and third-order distortion measurements were performed using a commercial GaAs MESFET as the control element. This device had measured values of pinch off voltage and open channel current of 2.0 V and 150 mA, respectively. Gate bias was applied through a 1 kΩ resistor and the power available from the 50 Ω source was kept less than 0 dBm to keep the device out of saturation. The value

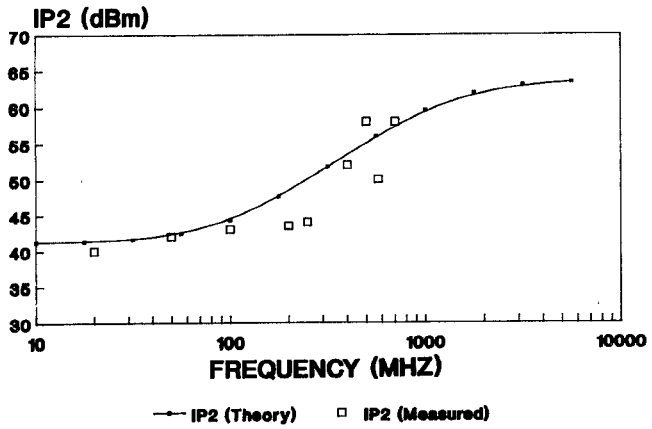

Fig. 7. Experimental measurements of second-order intercept point (IP2) in a series connected switch plotted versus frequency. Equation (7a) is plotted for comparison. The MESFET used exhibited a pinch off voltage of 2.5 V and an open channel current term of 150 mA.

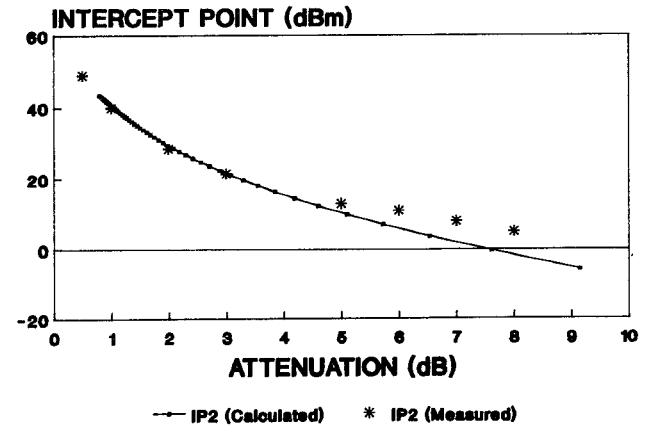

Fig. 8. Experimental measurements of second-order intercept point (IP2) versus attenuation level (A) in a series reflective attenuator measured at 410 MHz. Equation (9a) is plotted for comparison.

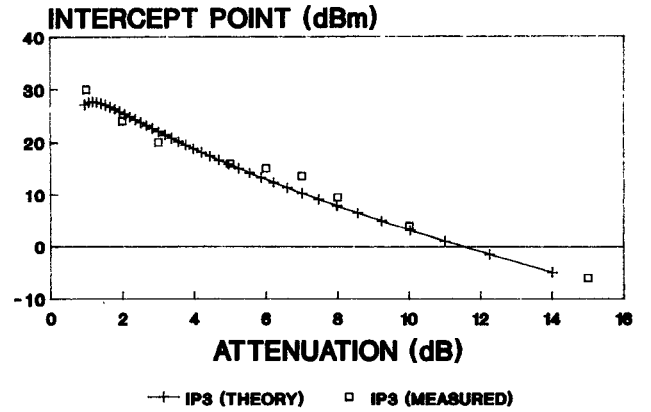

Fig. 9. Experimental measurements of third-order intercept point (IP3) versus attenuation level (A) in a series reflective attenuator measured at 410 MHz. Equation (9b) is plotted for comparison.

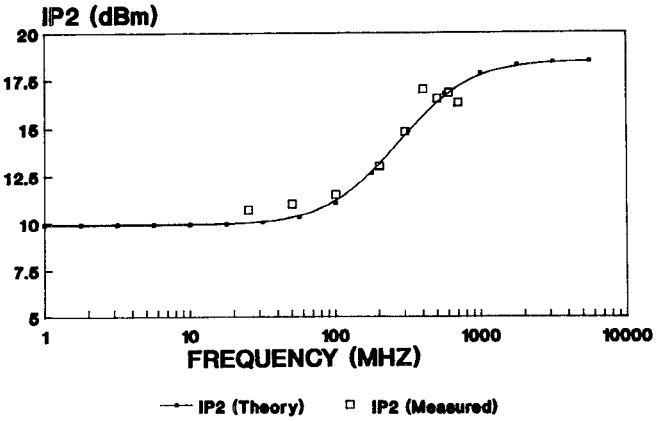

Fig. 10. Experimental measurements of second-order intercept point (IP2) versus frequency for a series reflective attenuator set for 4 dB attenuation. Equation (9a) is plotted for comparison.

of gate capacitance C_G was obtained from the manufacturer's specifications for the MESFET. The distortion test set and measurement techniques were similar to one previously described [12]. For the MESFET operating as a switch in its conducting state (zero gate–source voltage), IP2 was measured from frequencies of 20 to 700 MHz. These measured results are illustrated in Fig. 7, with (7a) plotted for comparison. At low frequencies, the increased distortion (low distortion intercept point) is caused by the MESFET being driven closer to saturation (and the resulting nonlinear operation) during the positive RF swing. As the frequency is increased beyond $1/2\pi R_G C_G$, the floating gate condition reduces the magnitude of V_{GS}, allowing more linear operation and an increase in the intercept point.

The distortion performance in a series reflective attenuator was also measured. As the dc gate–source voltage V_{GS0} approaches V_P, the MESFET channel is almost completely pinched off. This results in a large value of R_{ch} and hence a high circuit attenuation (A). This same operating point, however, also coincides with operation near the MESFET saturation point, a strongly nonlinear region of operation [1], [2]. The result is an increased level of distortion (a lowered intercept point) with increasing circuit attenuation. Figs. 8 and 9 show measured second- and third-order intercept point data plotted versus attenuation level at 410 MHz. Calculated second- and third-order intercept points using (9a) and (9b) are plotted in Figs. 8 and 9 for comparison. Note that for levels of attenuation greater than approximately 3 dB, IP3 is greater than IP2. This crossover attenuation level is a function of both I_P and V_P. The experimental data shown in Figs. 8 and 9 verify the large variation in intercept point in single MESFET attenuators.

Fig. 10 shows experimental measurements of IP2 versus frequency at a specific level of attenuation, with (9a) plotted for comparison. As in the switch case, IP2 shows an increase with frequency, with the greatest variation in the vicinity of F_G. However, the degree of increase in intercept point is smaller, only about 8 dBm at the 4 dB attenuation level. This variation of intercept with frequency will decrease even further at the highest levels of attenuation.

IV. Conclusions

The results of a nonlinear analysis have been used in determining the level of distortion generated by the MESFET in RF and microwave control applications. The fundamental conclusion reached is that distortion in MESFET control circuits is directly related to the pinch off

voltage and open channel current capacity. The results, applied to series connected MESFET switches and attenuators, show good agreement with experimental measurements and indicate that V_P and I_P affect distortion performance. In a MESFET switch, where the MESFET operates with zero dc gate voltage, large I_P MESFET's will show lower levels of distortion. A peak in the intercept point occurs for those MESFET's with pinch off voltages in the 2–3 V range. In a MESFET attenuator, there is a wide variation in distortion levels over a 10 dB range of attenuation. The distortion level may be minimized by reducing the open channel current capacity in this application. This reduction in I_P will, however, influence the minimum attenuation level obtainable in the attenuator circuit. In all cases, the distortion is the highest at low frequencies, lowering at frequencies significantly above the gate bias circuit cut off frequency, $1/2\pi R_G C_G$. The analytic expressions derived will now allow circuit designers to predict distortion levels in single MESFET control circuits. These expressions will also enable the device designer to modify the MESFET design for specific distortion requirements.

Acknowledgment

The author would like to thank the faculty and staff, especially M. Howes and R. Miles, of the Department of Electronic and Electrical Engineering and The Microwave Solid-State Group of the University of Leeds, Leeds, UK, for their help and assistance. Additional thanks go to C. Snowden and R. Pantoja of the Microwave Solid-State Group for their helpful discussions, and to G. Millington of the Group for help in assembling the measurement test set and obtaining the necessary components for the test fixtures. The author would also like to thank G. Hiller of the Semiconductor Products Division of M/A-Com, Inc., Burlington, MA, for our many interesting discussions on the general problem of distortion in RF and microwave control circuits.

References

[1] R. Gutmann and D. Fryklund, "Characterization of linear and nonlinear properties of GaAs MESFET's for broad-band control applications," *IEEE Trans. Microwave Theory Tech.*, vol. MTT-35, no. 5, pp. 516–520, May 1987.

[2] N. Jain and R. Gutmann, "Modeling and design of GaAs MESFET control devices for broad-band applications," *IEEE Trans. Microwave Theory Tech.*, vol. 38, no. 2, pp. 109–117, Feb. 1990.

[3] R. Gutmann and N. Jain, "Comments on GaAs MESFET baseband-to-microwave passive switches," *IEEE Trans. Microwave Theory Tech.*, vol. 37, no. 7, p. 1154, July 1989.

[4] R. Caverly, "Nonlinear distortion in gallium arsenide MESFET control and switch circuits," in *Proc. IEE Colloq. Nonlinear Model. Microwave Devices Circuits*, London, England, June 1990.

[5] C. Snowden, M. Howes, and D. Morgan, "Large signal modeling of GaAs MESFET operation," *IEEE Trans. Electron Dev.*, vol. ED-30, pp. 1818–1824, Dec. 1983.

[6] C. Snowden, "Computer-aided design of MMICs based on physical device models," *Proc. Inst. Elec. Eng.*, vol. 133, no. 5, pt. H, pp. 419–427, Oct. 1986.

[7] S. M. Sze, *Physics of Semiconductor Devices*, 2nd ed. New York: Wiley, 1981, 314–319.

[8] L. Chua and Y. Sing, "Nonlinear lumped circuit model of GaAs MESFET," *IEEE Trans. Electron Dev.*, vol. ED-30, no. 7, pp. 825–833, July 1983.

[9] M. Shur, "Analytical model of GaAs MESFETs," *IEEE Trans. Electron Dev.*, vol. 25, no. 6, pp. 612–618, June 1978.

[10] M. Schnidler, M. Miller, and K. Simon, "Reply to comments on GaAs baseband-to-microwave passive switches," *IEEE Trans. Microwave Theory Tech.*, vol. 37, no. 7, pp. 1154–1155, July 1989.

[11] G. Heiter, "Characterization of nonlinearities in microwave devices and systems," *IEEE Trans. Microwave Theory Tech.*, vol. MTT-21, p. 797, Dec. 1973.

[12] R. Caverly and G. Hiller, "Distortion in p-i-n diode control circuits," *IEEE Trans. Microwave Theory Tech.*, vol. MTT-35, pp. 492–501, May 1987.

[13] A. Gopinath and J. Rankin, "GaAs FET RF switches," *IEEE Trans. Electron Dev.*, vol. ED-32, no. 7, pp. 1272–1278, July 1985.

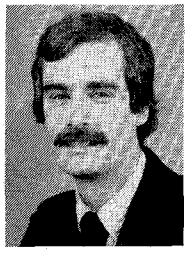

Robert H. Caverly (S'80–M'82) was born in Cincinnati, OH, in 1954. He received the M.S.E.E. and B.S.E.E. degrees from the North Carolina State University, Raleigh, in 1978 and 1976, respectively, and the Ph.D. degree in electrical engineering from The Johns Hopkins University, Baltimore, MD, in 1983.

He has been employed at Southeastern Massachusetts University, North Dartmouth, since 1983, where he is now an Associate Professor. He has been a consultant for M/A-COM, Inc. during that time. In 1990, he was a Visiting Research Fellow with the Microwave Solid-State Group at the University of Leeds, Leeds, UK.

In 1987, Dr. Caverly received the Dow Outstanding Young Faculty Award from the American Society of Engineering Education. In 1985, he was appointed Director of the university's Computer Aided Engineering Laboratory, and he is currently involved with the Massachusetts Microelectronics Center's educational activities. He is currently involved with nonlinear characterization of p-i-n diodes and MESFET's in the microwave and RF control environment.